Applied Computer Science, vol. 20, no. 2, pp. 43–59
doi: 10.35784/acs-2024-15

Submitted: 2024-03-12 | Revised: 2024-06-05 | Accepted: 2024-06-16

Keywords: optimal measurement time, CNC machine tool, machine learning methods

Jerzy JÓZWIK [0000-0002-8845-0764]*,
Magdalena ZAWADA- MICHAŁOWSKA [0000-0003-3330-6340]*,
Monika KULISZ [0000-0002-8111-2316]**, *Paweł TOMIŁO* [0000-0003-4461-3194]***,
Marcin BARSZCZ [0000-0002-9061-4414]****, *Paweł PIEŚKO* [0000-0002-4152-5159]*,
Michał LELEŃ [0000-0002-6398-4014]*, *Kamil CYBUL* [0009-0008-4321-3045]*****

MODELING OF OPTIMAL PROBE MEASUREMENT TIME ON A MACHINE TOOL USING MACHINE LEARNING METHODS

Abstract

This paper explores the application of various machine learning techniques to model the optimal measurement time required after machining with a probe on CNC machine tools. Specifically, the research employs four different machine learning models: Elastic Net, Neural Networks, Decision Trees, and Support Vector Machines, each chosen for their unique strengths in addressing different aspects of predictive modeling in an industrial context. The study examines the input parameters such as material type, post-processing wall thickness, cutting depth, and rotational speed over measurement time. This approach ensures that the models account for the variables that significantly affect CNC machine operations. Regression value, mean square error, root mean square error, mean absolute percentage error, and mean absolute error were used to evaluate the quality of the obtained models. As a result of the analyses, the best modeling results were obtained using neural networks. Their ability to accurately predict measurement times can significantly increase operational efficiency by optimizing schedules and reducing downtime in machining processes.

* Lublin University of Technology, Faculty of Mechanical Engineering, Department of Production Engineering Fundamentals, Poland, j.jozwik@pollub.pl, m.michalowska@pollub.pl, p.piesko@pollub.pl, m.lelen@pollub.pl
** Lublin University of Technology, Management Faculty, Department of Enterprise Organisation, Poland, m.kulisz@pollub.pl
*** Lublin University of Technology, Management Faculty, Department of Quantitative Methods, Poland, p.tomilo@pollub.pl
**** Lublin University of Technology, Electrical Engineering and Computer Science Faculty, Department of Computer Science, Poland, m.barszcz@pollub.pl
***** Lublin University of Technology, Doctoral School at the Lublin University of Technology, Poland, k.cybul@pollub.pl

1. INTRODUCTION

Workpiece probes, also known as touch probes, are now standard equipment on CNC machine tools. They are used to position the object in the working space of the machine and to measure the manufactured elements. Measurements of elements manufactured on CNC machines are performed both during and immediately after machining (Guiassa & Mayer, 2011; Kamieńska-Krzowska et al., 2007; Kwon, et al., 2006a). This makes it possible to check the conformity of the element before it is removed from the machine tool, which is much faster and cheaper than using coordinate measuring machines. It should be noted, however, that workpiece probe measurements are much less accurate than those made with CMMs. The uncertainty of measurement on a CNC machine using a touch probe is influenced by many factors, and determining it is a complex issue. Probe manufacturers typically specify a unidirectional repeatability of 2σ as a parameter to characterize the inaccuracy, which is a small component of the uncertainty budget. CNC machines use control and measurement systems for probe-based measurements, so the geometric and positioning accuracy of the machine, as well as the accuracy of the standards used in it, are much more critical to the accuracy of the measurements (Jacniacka & Semotiuk, 2011; Kwon, et al., 2006b; Sałamacha & Józwik, 2023). The authors of works (Blecha et al., 2022; Jacniacka et al., 2010) have experimentally estimated that the measurement uncertainty with probes does not exceed 2 μm. Given that this 2 μm uncertainty is within the manufacturing tolerances commonly used in the industry, it is considered to be very small. Therefore, it is critical to minimize the influence of external factors on the measurement results obtained on CNC machines. One such factor is the thermal expansion of the workpiece due to the heat generated during the cutting process.

Heat balance models in the cutting process have been developed and are well-known for many years (Olszak, 2008). In simplified terms, they assume that heat from the cutting zone is dissipated in fixed proportions respectively to the workpiece, chip, tool, and surroundings. In reality, the distribution of heat flow depends on various technological parameters used. In the context of post-machining thermal deformations of the workpiece, the most significant factor is the amount of heat delivered to it, which decreases with increased cutting speed and feed rate (Bobrov, 1975; Fleischer et al., 2007). The heat generated during the cutting process raises the temperature of the workpiece, affecting machining accuracy and tool wear (Wang et al., 2010). As a result of this heat, thermal deformations occur in both the workpiece and the tool. When measuring the accuracy of machined components, it is therefore crucial to understand the quantity and distribution of the process heat transferred to the workpiece. Several analytical studies aim to determine the amount of heat generated during the cutting process and its distribution, as well as its impact on machining accuracy (Li & Liang, 2006; Putz et al., 2016). Even slight thermal deformations can be the reason for errors that exceed the expected deviation values, particularly in precision and ultra-precision machining (Moriwaki et al., 1990; Wang et al., 2010).

The authors of paper (Jacniacka & Semotiuk, 2011) performed machining at relatively low cutting speeds (v_c = 80 m/min for steel and v_c = 400 m/min for aluminum alloy, respectively) and observed that the deformations caused by heat generated in the machining process are significant and cannot be ignored when measuring with workpiece probes. However, it should be noted that the use of High-Performance Cutting (HPC) techniques, due to the substantial cross-sections of the cut layer and the cutting speeds, reduces the

amount of heat transferred to the workpiece, which can affect the thermal deformations and the measurement accuracy of the workpiece.

In the literature (Kizaki et al., 2021; Shi et al., 2023; Weck et al., 1995), significant attention is devoted to machining errors arising from thermal deformations of machine tool elements, without considering the thermal deformations of the workpiece. In paper (Shi et al., 2023), thermal errors of the machine tool are analyzed and modeled based on the dimensional error of the machined parts. Measurements were conducted manually, with thermal errors of the machine tool being considered as the primary and practically the only factor affecting the value of the observed dimensional deviations.

Based on preliminary research, the results of which were published in (Kulisz et al., n.d.; Pieśko et al., 2023), it can be deduced that due to the heat absorbed by the workpiece and its thermal inertia, changes in the volume of the workpiece occur not only during the machining process, but also some time after its completion. Therefore, it is crucial to determine the appropriate time to begin measurements after machining has ended, so that changes in the dimensions of the machined element do not impact the accuracy of the measurement. In previous studies (Kulisz et al., n.d.), the optimal time for a given range of processing parameters was determined based on experimental results. The novelty of this research lies in using the results of earlier studies to create a model that predicts the time at which measurements can be made for a specified range of processing parameters. To this end, an algorithm utilizing machine learning methods (Elastic Net, Neural Networks, Decision Trees, and Support Vector Machines) was developed as part of the ongoing work. Machine learning methods, particularly those using artificial neural networks, are increasingly employed in various engineering issues (Arachchige et al., 2021; Biruk-Urban et al., 2023; Kulisz, et al., 2022a; 2022b; 2022c). Consequently, there arose the idea to use them to determine the optimal time to commence measurements with an inspection probe following the completion of machining.

2. METHODOLOGY

2.1. Experimental methodology

In order to obtain data for training an artificial neural network and then to validate the correct operation of the developed numerical model, experimental tests were carried out, including measurements of changes in temperature and geometry of the tested samples, according to the general scheme presented in Fig. 1. The tests were carried out on a test rig consisting of the following devices:

- AVIA VMC 800HS 3-axis machining center,
- Heidenhain TS 640 measuring probe,
- FLIR X6580sc thermal camera,
- Gocator 2400 laser line profile sensors.

The tests used samples in the form of cuboid solides made of aluminum alloy EN AW-2024 T351 and steel S235 with dimensions 105x33x50 mm (Fig. 2). Selected physical properties and chemical composition of the alloy EN AW-2024 T351 are summarized in Tab. 1. Tab. 2 shows the chemical composition and properties of S235 steel.

The X6580sc thermal imaging camera was used to measure the temperature and analyze it's distribution on the sample surface (Fig. 3). Thermographic measurements are sensitive to any type of interference in the form of reflections that occur on metallic shiny surfaces. In order to eliminate these reflections and increase the emissivity coefficient, the surface of the sample was covered with black matte paint with a known emissivity (0.95).

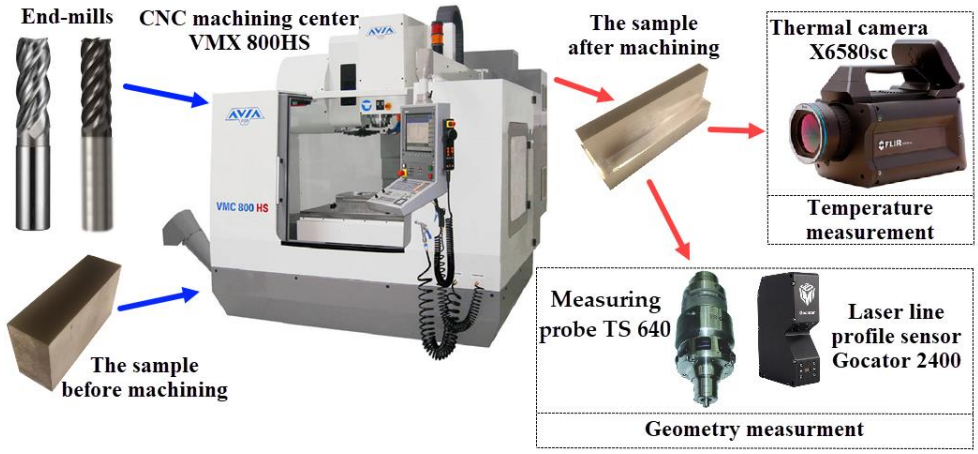

Fig. 1. The plan of the experiment

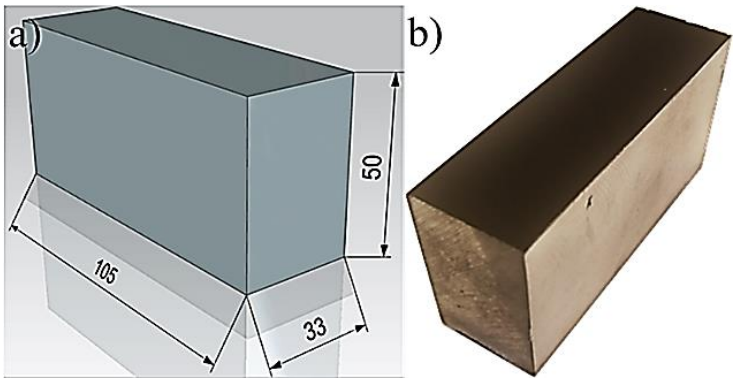

Fig. 2. Test samples: a) view of the model with dimensions, b) view of the sample

Tab. 1. Chemical composition and selected properties of an alloy AW-2024 T351 (Weck et al., 1995)

The concentration of chemical elements [%]										
Si	*Fe*	*Mg*	*Cu*	*Mn*	*Zn*	*Li*	*Ag*	*Cr*	*Zr +Ti*	*others*
≤0.5	≤0,5	1.5	4.2	0.6	≤0.25	-	-	≤0.1	≤0.2	≤0.15
Selected physical properties										
Young's modulus E [GPa]	*Tensile strength R_m [MPa]*	*Percentage elongation A [%]*	*Specific heat at 20 °C [J/kgK]*	*Coefficient of thermal expansion at 20°C [µm/mK]*	*Thermal conductivity λ [W/mK]*					
70	430	7	874	23	121					

Tab. 2. Chemical composition and selected properties of a steel S235 (Weck et al., 1995)

The concentration of chemical elements [%]					
C	*Mn*	*P*	*S*	*N*	*Cu*
≤0.17	≤1.40	≤0.035	≤0.035	≤0.12	≤0.55
Selected physical properties					
Young's modulus E [GPa]	*Tensile strength R_m [MPa]*	*Elongation at break A [%]*	*Specific heat at 20 °C [J/kgK]*	*Coefficient of thermal expansion at 20°C [µm/mK]*	*Thermal conductivity λ [W/mK]*
205	360-510	25	490	11	58

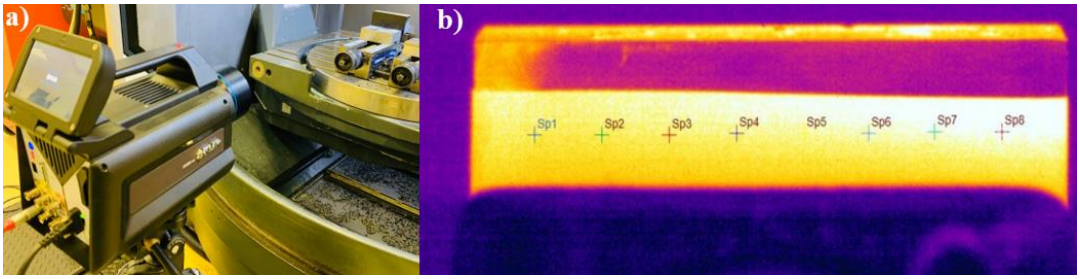

Fig. 3. Measuring temperature using a thermal camera: a) measurement method, b) localization of measurement points

A TS 640 touch probe was used to measure the sample geometry. In addition, the probe measurement results were verified using a Gocator 2400 laser line profile sensor. Eight measurement points were selected along the laser beam, corresponding to the temperature measurement points. The method of performing the geometric measurements is shown is shown in Figure 4. A four-thooth carbide end-mill from SGS Tools with the symbol 44630 was used for machining aluminum alloy, and a six-thooth coated carbide end-mill from SECO Tools with the symbol JS520120D2C.0Z6-NXT was used for machining steel.

Fig. 4. Geometry measurement with a Gocator 2400 laser line profile sensor and TS 640 touch probe

2.2. Modeling methodology

The variable input parameters of the modeling process were:

– the type of material being analyzed r_m (AW 2024 alloy - 1, Steel S235 - 2);

– the post-processing wall thickness g (ranging from 1 mm to 30 mm);
– the depth of cut a_p (a_p = 10 mm; a_p = 20 mm);
– the rotational speed n (n = 2500 rpm; n = 15000 rpm).

The output parameter of the models was the time after which it is possible to measure the processed object (measurement time). Four distinct machine learning methods—Elastic Net, Neural Networks (NN), Decision Trees, and Support Vector Machines (SVM)—were selected for the modeling of measurement time to capitalize on their unique strengths and approaches. The methodology for the development of this research is shown in the flowchart below (Fig. 5). The dataset, which consisted of 46 observations, was partitioned into a 75% slice for training and a 25% slice for testing, deliberately forgoing a validation subset due to the dataset's constrained size.

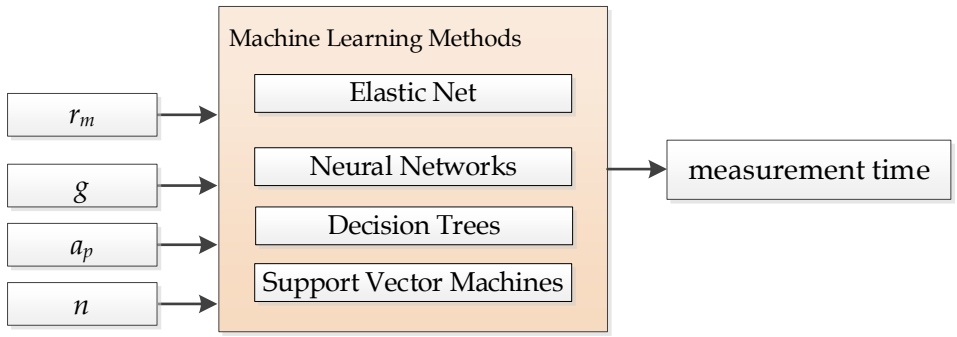

Fig. 5. Flowchart of the research methodology

Elastic Net, a regularized regression method that combines L1 and L2 penalization, was chosen for its robustness in feature selection, particularly useful in scenarios with multiple correlated features or more features than observations. It has been utilized to mitigate the issues of multicollinearity and to diminish the influence of less significant variables. Neural Networks, known for their powerful function approximation capabilities, were employed to model the complex and non-linear relationships that exist between the inputs and outputs. They were leveraged for their capacity to learn intricate patterns within high-dimensional spaces, which is essential when the relationship between parameters and outcome is not straightforward. Decision Trees were implemented to segment the predictor space into simple regions, providing a model structure that can be visualized and understood through if-then-else decision rules. Their transparent and interpretable nature was deemed beneficial for situations where the clarity of the decision-making process is paramount. Support Vector Machines were used for their proficiency in classification and regression tasks, especially due to their kernel functions that handle high-dimensional spaces well, even with non-linearly separable data. SVMs are characterized by their focus on maximizing the margin in the feature space, a feature that often results in a model with high generalization ability and robustness against overfitting.

The collective utilization of these methods ensured a comprehensive examination of the modeling task. By comparing their performances, it was possible to ascertain the most fitting method for accurately predicting the measurement time, thereby identifying the optimal solution for the specific requirements of precision and computational efficiency in the given context.

ElasticNet is a regression method that incorporates regularization to improve stability when dealing with noisy data. It relies on a model where the dependent variable matrix is determined through a set of predictor variables, influenced by a noise component. This technique merges the concepts of L1 regularization, popularized by Tibshirani as LASSO (Least Absolute Shrinkage and Selection Operator), with L2 regularization, which is central to ridge regression methods. Through this hybrid approach, ElasticNet is able to reap the advantages of both regularization methods, providing a versatile and potent tool for various data analysis situations. In the current model configuration, it's presumed that the response variables follow a Gaussian distribution, a standard assumption for regression models. A five-fold cross-validation technique was applied to evaluate the model's consistency and to prevent it from matching the noise in the training data too closely. The model explored a spectrum of alpha values from 0.1 up to 1.0, alongside a series of lambda values—these being 0.00001, 0.0001, 0.001, 0.01, 0.1, and 1. This iterative process was aimed at locating the alpha and lambda pair that would result in the lowest possible MSE. Post-identification, the chosen model was put through its paces with several statistical measures, including the RMSE, RIE, MAPE, and MAE (described below), to evaluate its predictive performance thoroughly.

In the construction of the Neural Networks model, a single-layered network was employed, which is renowned for its proficiency in delineating intricate patterns with minimal computational demand. The neuron count in the hidden layer was dynamically adjusted, within a scope of 2 to 15, to fine-tune the model, a process guided by iterative experimentation to establish an optimal equilibrium between the model's structural complexity and its predictive prowess. The choice of Bayesian regularization for training was deliberate, aimed at enhancing generalization by tempering overfitting, particularly relevant given the dataset's limited volume of 46 entries. Model training was diligently managed to prevent overfitting, a frequent challenge in machine learning where a model overly aligns with the training data and underperforms on new, unseen data. To counter this, training was halted after six successive rises in validation error, or if there was no further reduction in error. This method, known as "early stopping," helps to mitigate overfitting by ceasing the training when the model's performance on the validation set starts to decline.

In the methodology for Decision Tree modeling, an ensemble approach was leveraged. A comprehensive sweep of the number of trees, from a minimum of 50 to a maximum of 500 with increments of 5, was systematically executed to determine the optimal forest size. The aim was to discern a sweet spot where the model complexity and prediction error, measured by Mean Squared Error, were balanced. The analytical process culminated in identifying the model configuration that yielded the lowest MSE, thereby nominating it as the most efficient. The key characteristics of this model were then systematically reported, outlining the number of trees and corresponding error metrics.

In the methodology for Support Vector Machine (SVM) modeling, the emphasis was placed on hyperparameter optimization to refine the regression capabilities of the model. The hyperparameters subjected to optimization included the Box Constraint, Kernel Scale, and Epsilon. These were not arbitrarily chosen; their ranges were systematically defined to explore a space conducive to robust model performance. Bayesian optimization was utilized for its strategic exploration of the hyperparameter space, seeking to minimize cross-validation loss within a 5-fold framework. This process was designed to be exhaustive within the predefined parameter bounds: the Box Constraint was varied to manage the trade-off

between classification margin and misclassification rate, the Kernel Scale to adjust the fit of the data in the feature space, and Epsilon to control the width of the margin within which no penalty is given to errors in the SVM's output. Once the optimal hyperparameters were determined, their values and the corresponding minimum loss were recorded. This information was crucial for understanding the configuration of the most effective SVM model within the given parameter bounds.

Evaluating a model's performance and determining its validity and appropriateness are primary objectives of model comparisons. It is crucial to use evaluation metrics for models to estimate their optimal forecasting performance, particularly in the case of machine learning-based methods. Therefore, the qualitative metrics presented in Tab. 3 were used in the conducted research.

Tab. 3. Quality indicators for evaluating machine learning models

Quality indicators	Formula	Explanations of the symbols
Regression value R	$R(y', y^*) = \frac{cov(y', y^*)}{\sigma_{y'}\sigma_{y^*}}$, $R\epsilon < 0,1 >$	$\sigma_{y'}$ - standard deviation of the real data, σ_{y^*} - standard deviation of the predicted data, y_i - the real data, $\hat{y}_i$ - the value of the data for the i-th observation obtained from the model.
Mean Squared Error (MSE)	$MSE = \frac{1}{n}\sum_{i=1}^{n}(\hat{y}_i - y_i)^2$	
Root Mean Square Error (RMSE)	$RMSE = \sqrt{\frac{\sum_{i=1}^{n}(y_i - \hat{y}_i)^2}{n}}$	
Mean Absolute Percentage Error (MAPE)	$MAPE = \frac{1}{n}\sum_{i=1}^{n}\left\|\frac{y_i - \hat{y}_i}{y_i}\right\|$	
Mean Absolute Error (MAE)	$MAE = = \frac{1}{N}\sum_{i=1}^{N}\|y_i - \hat{y}_i\|$	

3. RESULTS

3.1. ElasticNet model

The best ElasticNet model was obtained for alpha = 1 and lambda = 0.00001. The evaluation of the complexity and fit of the model depending on the MSE obtained is shown in Figure 6. Fig. 6a illustrates the Mean Squared Error (MSE) variation with respect to different Alpha values for each specified Lambda value, indicating the model's sensitivity to the Alpha parameter in the regularization process. Fig. 6b shows the MSE in relation to varying Lambda values for each predefined Alpha, demonstrating how the strength of regularization impacts model performance. Finally, Fig. 6c provides a detailed view of MSE trends against Lambda values when Alpha is fixed at 1, with the optimal model configuration marked by a red star, representing the lowest MSE achieved. Collectively, these plots are crucial for fine-tuning the balance between model complexity and its ability to generalize, utilizing an early stopping strategy to prevent overfitting to the training data.

The results of all qualitative parameters for the best model are shown in Table 4. With an alpha value of 1, the model tended toward lasso regression, emphasizing feature selection. The lambda value of 0.00001 indicated a preference for less regularization, allowing for

greater model flexibility. The model achieved a MSE = 25.2284, indicating a good fit to the data. The RMSE was 5.0227, providing a realistic measure of prediction dispersion. The RIE was 0.1757, indicating accurate predictions, and the MAPE was 0.253, indicating high prediction accuracy. Finally, the MAE was 3.586, further confirming the model's predictive accuracy. Figure 7 shows regression graphs for the total set for ElasticNet model.

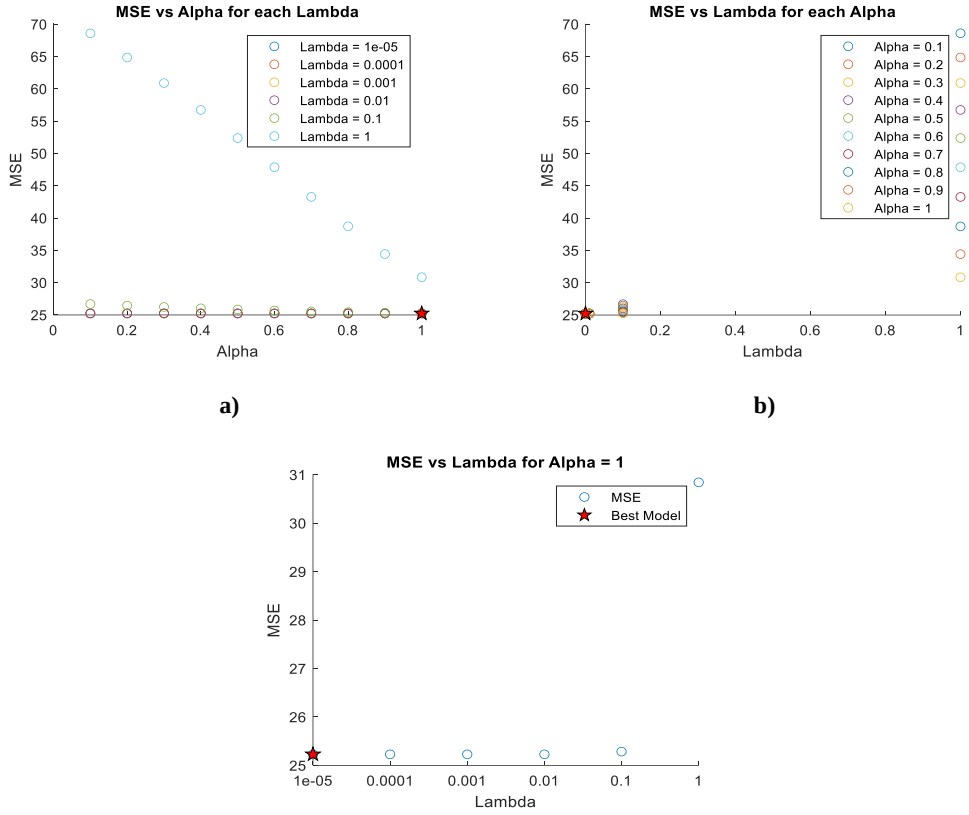

Fig. 6. Model Complexity and Fit Assessment through MSE, comparing a) alpha variations per Lambda level, b) Lambda changes per Alpha setting, and c) Lambda impact when Alpha equals 1, with the best model highlighted

Tab. 4. Results of ElasticNet quality indicators

Quality indicators	Regression value (all data)	MSE	RMSE	RIE	MAPE	MAE
ElasticNet	0.93235	25.2284	5.0227	0.1757	0.253	3.586

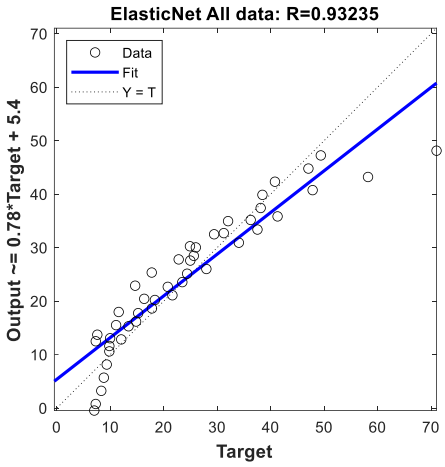

Fig. 7. Regression statistics for the total set for ElasticNet

3.2. Neural Networks model

The artificial neural networks using the Bayesian Regularization training algorithm achieved the best results with 10 neurons in the hidden layer, obtained after 280 epoch. The training results of this network are presented in Table 5.

Tab. 5. Results of neural network training

Training algorithm	Bayesian Regularization
Epoch	280
Performance	1.6
Best training performance	1.5985 at epoch 60
Gradient	0.55

Network quality indicators are presented in Table 6. Figure 8 depicts the training and testing MSE over the course of 280 epochs during a machine training model training process. The blue line represents the MSE for the training set, and the red line shows the MSE for the testing set. The dotted line labeled 'Best' indicates the epoch where the best performance on the validation set was achieved. The best training performance, with an MSE of 1.5985, was reached at epoch 60.

Tab. 6. Results of neural network quality indicators

Quality indicators	Regression value (all data)	MSE	RMSE	RIE	MAPE	MAE
Neural Network	0.99637	1.6285	1.2761	0.0447	0.0453	0.9472

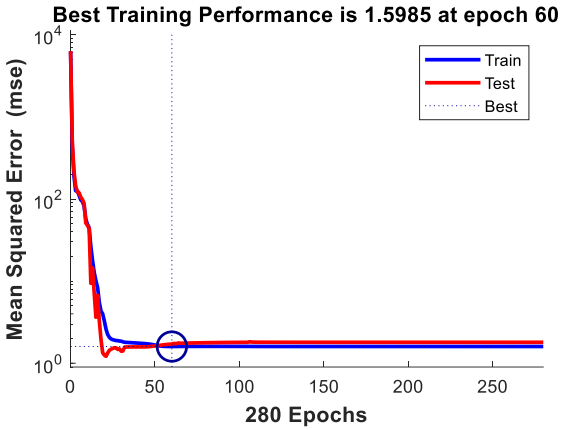

Fig. 8. The best training performance for the NN model

Additionally, Figure 9 presents regression graphs, with regression statistics showing an overall R-value of 0.99637 for the entire dataset. These charts facilitate the evaluation of the model's fit at various stages of the training process, demonstrating the model's accuracy in predicting values compared to the actual data in each set.

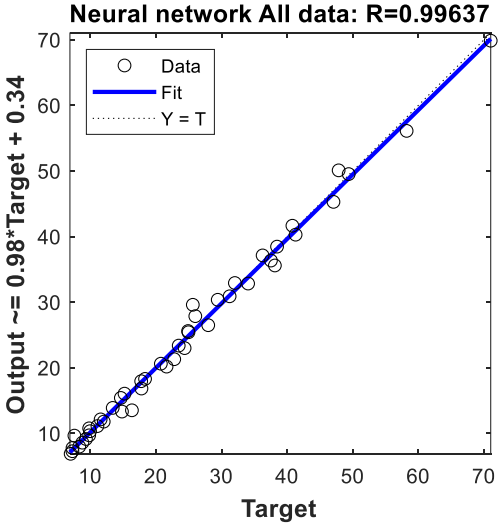

Fig. 9. Regression statistics for the total set for neural network

3.3. Decisions Trees model

The next method examined for modeling was the use of decision trees (DT). This approach entailed adjusting the quantity of trees from a minimum of 50 to a maximum of 500, in increments of 5 trees. Optimal results from DT modeling were achieved with a configuration of 290 trees. Figure 10 illustrates the MSE associated with various tree counts in the Decision Tree model.

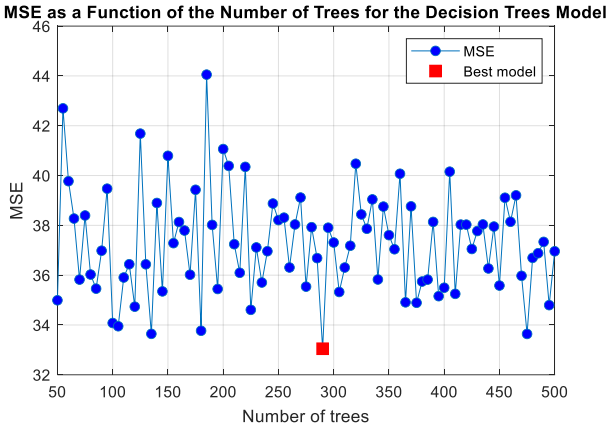

Fig. 10. MSE as a Function of the Number of Trees for the Decision Trees Model

Table 7 presents the outcomes of all qualitative metrics for the optimal Decision Trees model (290 trees). The model attained a MSE of 33.0463, which suggests a satisfactory alignment with the dataset. The RMSE stood at 5.7485, offering a practical estimation of the spread in prediction. The RIE was measured at 0.2011, reflecting precise predictions, while the MAPE at 0.2281 denoted a high level of predictive accuracy. Additionally, the MAE recorded at 4.0104, further verifies the model's precision in prediction. Figure 11 illustrates the regression plots for the entire dataset using the Decision Trees model.

Tab. 7. Results of Decision Trees quality indicators

Quality indicators	Regression value	MSE	RMSE	RIE	MAPE	MAE
Decision Trees	0.95369	33.0463	5.7485	0.2011	0.2281	4.0104

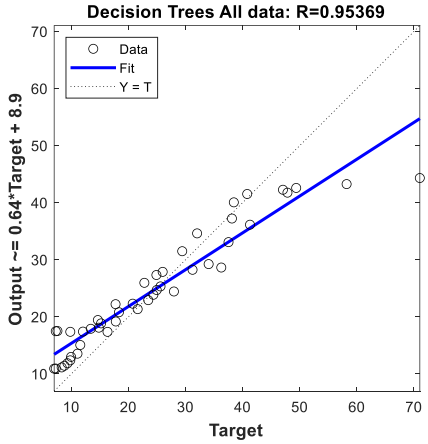

Fig. 11. Regression statistics for the total set for Decision Trees

3.4. Support Vector Machines model

The optimal Support Vector Machines regression model was determined through a hyperparameter optimization process, which completed after evaluating 30 different

configurations over a total elapsed time of 26.5751 seconds. The optimization aimed to minimize the cross-validation loss over a 5-fold partition of the data. The best-performing model, observed through the cross-validation process, achieved a loss of 3.3763. The hyperparameters of this model are presented in Table 8.

Tab. 8. The hyperparameters of SVM model

The hyperparameters	Support Vector Machines
Box Constraint (C)	40.492
Kernel Scale (σ)	0.78498
Epsilon (ε)	1.8291

These parameters were found to provide the most suitable balance between model complexity and generalization capability, as per the cross-validation metric used for evaluation. The Box Constraint controls the trade-off between allowing training errors and forcing rigid margins, the Kernel Scale defines the scale of the Gaussian kernel function, and the Epsilon sets the margin of tolerance where no penalty is given to errors.

Table 9 presents the outcomes of all qualitative metrics for the optimal SVM model. The regression value of 0.93963 suggests a strong predictive relationship, and the other metrics provide a comprehensive overview of the model's error characteristics, with the MSE being 26.4916, RMSE at 5.1470, RIE at 0.1801, MAPE at 0.2343, and MAE at 3.4969. Figure 12 illustrates the regression plots for the entire dataset using the best SVM model.

Tab. 9. Results of SVM quality indicators

Quality indicators	Regression value	MSE	RMSE	RIE	MAPE	MAE
SVM	0.93963	26.4916	5.147	0.1801	0.2343	3.4969

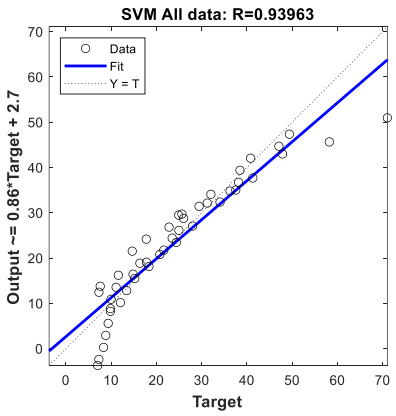

Fig. 12. Regression statistics for the total set for the best SVM model

3.5. Comparison of the obtained models

The performance comparison of the models: ElasticNet, neural network with Bayesian regularization training algorithm, decision trees and SVM is described in detail in Table 10.

Tab. 10. Comparison quality indicators of the obtained models

Quality indicators	ElasticNet	Neural Network	Decision Trees	SVM
Regression value (all data)	0.93235	0.99637	0.95369	0.93963
MSE	25.2284	1.6285	33.0463	26.4916
RMSE	5.0227	1.2761	5.7485	5.1470
RIE	0.1757	0.0447	0.2011	0.1801
MAPE	0.253	0.0453	0.2281	0.2343
MAE	3.586	0.9472	4.0104	3.4969

When comparing the performance metrics of machine learning models, key indicators provide insight into their predictive accuracy and generalizability. The regression value is indicative of how well the model fits the data, with values closer to 1 suggesting a better fit. The Neural Network stands out with a regression value nearly reaching perfection at 0.99637, whereas other models like Elastic Net, Decision Trees, and SVM demonstrate strong fits as well, with values above 0.93.

For error-based metrics, MSE and RMSE are critical. They reflect the average squared difference and square root of this difference between the predicted and actual values, respectively. Lower values are preferred, indicating higher accuracy. The Neural Network excels with the lowest MSE and RMSE, indicating precise predictions, while the Decision Trees lag with the highest values, suggesting less precision. Elastic Net and SVM fall in between, offering a moderate level of error in predictions.

RIE and MAPE measure the relative errors and are significant in contexts where the scale of the error in proportion to the true value is crucial. Here again, the Neural Network achieves the lowest RIE and MAPE, implying it is most effective in capturing the relative trends in the data. The Elastic Net and SVM have moderate values, and Decision Trees have higher RIE and MAPE values, indicating a greater level of relative error.

Lastly, the MAE measures the average absolute difference between predicted and actual values, giving a straightforward representation of error magnitude. The Neural Network achieves the lowest MAE, further solidifying its position as the most accurate model. Conversely, the SVM has the highest MAE, suggesting that on average, its predictions are further from the actual values than those of the other models.

In summary, each quality indicator across the models paints a comprehensive picture: the Neural Network is consistently superior across all metrics, while Decision Trees generally underperform compared to the rest. Elastic Net and SVM occupy the middle ground, with strengths and weaknesses that may make them suitable for particular scenarios or preferences.

The predicted time after which a measurement can be taken of an object processed by an inspection probe on a CNC machine for all analyzed cases obtained using the neural network model is shown in Fig. 13. The results indicate that the obtained neural network model can effectively predict the time after which a measurement of the processed object can be performed.

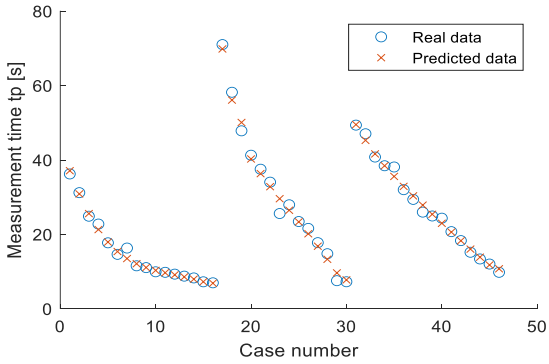

Fig. 13. Comparison of real and predicted data

A careful and thorough analysis of the model-generated data and the real data usually shows a close correlation between the actual and predicted values. There are, however, notable deviations where the predicted values either overestimate or underestimate the actual times. For instance, case 17 shows the largest real measurement time of 71.03 seconds, with the prediction slightly underestimating at 69.9 seconds. This small discrepancy suggests that while the neural network model has captured the overall trend, individual predictions could be fine-tuned for greater accuracy. Conversely, case 29 shows an overestimation in the predicted value, where the real data records a measurement time of 7.57 seconds, and the model predicts 9.1 seconds. This kind of overestimation could be critical in planning the workflow of CNC machining processes, as it may suggest longer waiting times for quality inspection than necessary. The bulk of the predictions aligns closely with the actual data, as cases 1 through 16 and 30 through 46 exhibit minor differences between the real and predicted times. This accuracy in prediction demonstrates the neural network's potential as a robust tool for forecasting measurement times in a manufacturing environment, which can significantly aid in enhancing operational efficiency and scheduling.

Overall, the model shows a high degree of predictive power and could be effectively integrated into a CNC machining workflow to anticipate post-processing inspection times, thereby optimizing the process and reducing downtime.

4. CONCLUSIONS

The primary focus is on the utilization of four distinct machine learning techniques: Elastic Net, Neural Networks, Decision Trees, and Support Vector Machines (SVM). Each method was selected to leverage its unique capabilities in handling the intricacies of predictive modeling in an industrial setting.

The modeling involved variable input parameters based on the type of material, the thickness of the material after processing, the depth of cut, and the rotational speed. These parameters significantly influence the measurement time, which is critical for optimizing CNC machine operations.

Based on the detailed analysis of the models using Elastic Net, Neural Networks, Decision Trees, and SVM for predicting measurement time on a CNC machine tool, the

Neural Networks model outperformed the others. This conclusion is drawn from comparing several key performance indicators outlined in the study.

The Neural Networks model achieved the highest regression value among all models at 0.99637, indicating a near-perfect fit. This model also exhibited the lowest MSE at 1.6285 and the lowest RMSE at 1.2761, suggesting its superior accuracy in predicting measurement times. Furthermore, the Neural Networks model demonstrated the lowest RIE and MAPE, at 0.0447 and 0.0453 respectively, which signifies its high reliability in producing precise predictions compared to the actual data.

In terms of practical industrial applications, the Neural Networks model's robust performance makes it exceptionally suitable for integration into CNC machining operations. Its ability to accurately predict measurement times can significantly enhance operational efficiency by optimizing the scheduling and reducing downtime. The model's precision in capturing complex relationships between multiple input parameters and the measurement time is particularly beneficial for maintaining high-quality standards and improving throughput in manufacturing processes.

The direction of further research will involve the development of a methodology for creating such models. The primary limitation of this study is its focus on a single case study, which may restrict the generalizability of the findings to other cases.

Funding

This work was prepared within the project PM/SP/0063/2021/1 titled "Innovative measurement technologies supported by digital data processing algorithms for improved processes and products", financed by the Ministry of Education and Science (Poland) as a part of the Polish Metrology Programme.

Conflicts of Interest

The authors declare no conflicts of interest.

REFERENCES

Arachchige, A., Sugathadasa, R., Herath, O. & Thibbotuwawa, A. (2021). Artificial neural network based demand forecasting integrated with federal funds rate. *Applied Computer Science*, *17*(4), 34–44. https://doi.org/10.23743/ACS-2021-27

Biruk-Urban, K., Zagórski, I., Kulisz, M. & Leleń, M. (2023). Analysis of vibration, deflection angle and surface roughness in water-jet cutting of AZ91D magnesium alloy and simulation of selected surface roughness parameters using ANN. *Materials*, *16*(9), 3384. https://doi.org/10.3390/MA16093384

Blecha, P., Holub, M., Marek, T., Jankovych, R., Misun, F., Smolik, J. & Machalka, M. (2022). Capability of measurement with a touch probe on CNC machine tools. *Measurement*, *195*, 111153. https://doi.org/10.1016/J.MEASUREMENT.2022.111153

Bobrov, V. F. (1975). *Basics of metal cutting theory*. Mechanical engineering.

Fleischer, J., Pabst, R. & Kelemen, S. (2007). Heat flow simulation for dry machining of power train castings. *CIRP Annals*, *56*(1), 117–122. https://doi.org/10.1016/J.CIRP.2007.05.030

Guiassa, R. & Mayer, J. R. R. (2011). Predictive compliance based model for compensation in multi-pass milling by on-machine probing. *CIRP Annals*, *60*(1), 391–394. https://doi.org/10.1016/J.CIRP.2011.03.123

Jacniacka, E. & Semotiuk, L. (2011). Odkształcenia cieplne a niedokładność pomiaru sondą przedmiotową. *Pomiary Automatyka Kontrola*, *57*(9), 985–988.

Jacniacka, E., Semotiuk, L. & Pieśko, P. (2010). Niepewność pomiaru wewnątrzobrabiarkowego systemu pomiarowego z zastosowaniem sondy OMP 60. *Przegląd Mechaniczny*, *6*, 36–42.

Kamieńska-Krzowska, B., Semotiuk, L. & Czerw, M. (2007). Analiza możliwości zastosowania sondy przedmiotowej do kontroli czynnej na pionowym centrum obróbkowym FV 580A. *Acta Mechanica et Automatica*, *1*(2), 19–24.

Kizaki, T., Tsujimura, S., Marukawa, Y., Morimoto, S. & Kobayashi, H. (2021). Robust and accurate prediction of thermal error of machining centers under operations with cutting fluid supply. *CIRP Annals*, *70*(1), 325–328. https://doi.org/10.1016/J.CIRP.2021.04.074

Kulisz, M., Zagórski, I., Józwik, J. & Korpysa, J. (2022a). Research, modelling and prediction of the influence of technological parameters on the selected 3D roughness parameters, as well as temperature, shape and geometry of chips in milling AZ91D Alloy. *Materials*, *15*(12), 4277. https://doi.org/10.3390/ma15124277

Kulisz, M., Zagórski, I., Weremczuk, A., Rusinek, R. & Korpysa, J. (2022b). Analysis and prediction of the impact of technological parameters on cutting force components in rough milling of AZ31 magnesium alloy. *Archives of Civil and Mechanical Engineering*, *22*, 1. https://doi.org/10.1007/s43452-021-00319-y

Kulisz, M., Józwik, J., Barszcz, M., Pieśko, P., Zawada- Michałowska, M. & Leleń, M. (n.d.). Process analysis, optimization and modeling of time measuring of the workpiece using an inspection probe on a CNC machine tool. *Metrology and Hallmark, Central Office of Measures*. In press.

Kulisz, M., Kujawska, J., Aubakirova, Z., Zhairbaeva, G. & Warowny, T. (2022c). Prediction of the compressive strength of environmentally friendly concrete using artificial neural network. *Applied Computer Science*, *18*(4), 68–81. https://doi.org/10.35784/ACS-2022-29

Kwon, Y., Jeong, M. K. & Omitaomu, O. A. (2006a). Adaptive support vector regression analysis of closed-loop inspection accuracy. *International Journal of Machine Tools and Manufacture*, *46*(6), 603–610. https://doi.org/10.1016/J.IJMACHTOOLS.2005.07.011

Kwon, Y., Tseng, T. L. & Ertekin, Y. (2006b). Characterization of closed-loop measurement accuracy in precision CNC milling. *Robotics and Computer-Integrated Manufacturing*, *22*(4), 288–296. https://doi.org/10.1016/J.RCIM.2005.06.002

Li, K.-M. & Liang, S. Y. (2006). Modeling of cutting temperature in near dry machining. *Journal of Manufacturing Science and Engineering*, *128*(2), 416–424. https://doi.org/10.1115/1.2162907

Moriwaki, T., Horiuchi, A. & Okuda, K. (1990). Effect of cutting heat on machining accuracy in ultra-precision diamond turning. *CIRP Annals*, *39*(1), 81–84. https://doi.org/10.1016/S0007-8506(07)61007-5

Olszak, W. (2008). *Obróbka Skrawaniem*. WNT.

Pieśko, P., Zawada-Michałowska, M. & Józwik, J. (2023). Influence of thermal deformations on accuracy measurement with an inspection probe. *2023 IEEE 10th International Workshop on Metrology for AeroSpace (MetroAeroSpace)* (pp. 280–284). IEEE. https://doi.org/10.1109/METROAEROSPACE57412.2023.10190043

Putz, M., Schmidt, G., Semmler, U., Oppermann, C., Bräunig, M. & Karagüzel, U. (2016). Modeling of heat fluxes during machining and their effects on thermal deformation of the cutting tool. *Procedia CIRP*, *46*, 611–614. https://doi.org/10.1016/J.PROCIR.2016.04.046

Sałamacha, D. & Józwik, J. (2023). Evaluation of measurement uncertainty obtained with a tool probe on a CNC machine tool. *MANUFACTURING TECHNOLOGY*, *23*(4), 513–524. https://doi.org/10.21062/mft.2023.051

Shi, H., Xiao, Y., Mei, X., Tao, T. & Wang, H. (2023). Thermal error modeling of machine tool based on dimensional error of machined parts in automatic production line. *ISA Transactions*, *135*, 575–584. https://doi.org/10.1016/J.ISATRA.2022.09.043

Wang, S., To, S., Chan, C. Y., Cheung, C. F. & Lee, W. B. (2010). A study of the cutting-induced heating effect on the machined surface in ultra-precision raster milling of 6061 Al alloy. *International Journal of Advanced Manufacturing Technology*, *51*, 69–78. https://doi.org/10.1007/s00170-010-2613-7

Weck, M., McKeown, P., Bonse, R. & Herbst, U. (1995). Reduction and compensation of thermal errors in machine tools. *CIRP Annals*, *44*(2), 589–598. https://doi.org/10.1016/S0007-8506(07)60506-X